Design of 3D light emitting diodes based on nanoporous metal / polymer bulk junction composites & Synthesis of silver nanoparticles

Ewout Lubberman
s1892002

A thesis presented for the degree of
Bachelor of Science in Applied Physics

rijksuniversiteit
groningen

Department of Materials science
University of Groningen
Supervisors: Dr. Ir. E. Detsi & Prof. Dr. J.T.M. De Hosson
Date: 23 december 2013

Design of 3D light emitting diodes based on nanoporous metal / polymer bulk junction composites
&
Synthesis of silver nanoparticles

Ewout Lubberman

Abstract

The first part of this thesis focuses on the design and testing of an organic light emitting device (OLED) with a three dimensional geometry. 3D metal / polymer bulk junctions were grown inside the pores of nanoporous gold (NPG) by using electrochemical deposition and electrochemical polymerization. Junctions containing zinc oxide, polyaniline and poly(3,4-ethylenedioxy-thiophene) were evaluated by comparing light emission, current-voltage (I-V) characteristics, surface roughness and UV/Vis spectra. 2D and semi-3D devices were tested and results are compared to a conventionally prepared 2D reference device. In order to complete the transition from 2D to 3D OLED's, future work is required to find a suitable emission layer for the 3D device. The second part of this research thesis deals with the synthesis of silver nanoparticles. These particles were grown using electrochemical deposition and polyol synthesis. The particles morphology is studied at different angles with a scanning electron microscope (SEM). These pictures are used to calibrate a novel 3D digital image correlation algorithm.

Contents

Chapter 1

Design of 3D light emitting devices based on nanoporous metal / polymer bulk junction composites

1.1 | Motivation and goals

In times of an ever-growing global demand for affordable energy, much of today's research effort focuses on new ways to meet that demand. One of the most promising areas in that field is that of organic semiconductors: using cheap plastics to make devices such as light emitting devices (LEDs), transistors and solar cells. This thesis focuses on the transition of LEDs from a 2D geometry to 3D, by making devices inside the pores of nanoporous metals. Using the chemical process of dealloying [1], the least noble constituent of metal alloys are diluted. This leaves nanoporous metals with a greatly enhanced surface area, up to 5.10^4 m^2 kg^{-1} [2] depending on the pore size. The light emitting capacity of LEDs relates directly to its active surface area, so the 2D to 3D transition can potentially lead to an enormous leap in light output. Conventional LEDs consist of a multi-layer junctions, so growing thin films of different materials inside the pores of nanoporous materials will be necessary. This is at itself an interesting procedure, for exciting results in the mechanical behaviour of nanoporous metals have been demonstrated using a single polymeric coating [3] [4] [5].

1.2 | Theory

Organic light emitting devices and electroluminescent polymers

In the 1970s, MacDiarmid et al. [6] [7] discovered electrical conductivity in organic materials for the first time. The discovery of electroluminescent polymers (Burroughes et al. [8]) in the 1990s led to the exciting new field of organic light emitting devices (OLEDs). Suddenly it became possible to combine the good mechanical properties of polymers with their easy processability and low costs for a range of new devices.

In traditional polymers, the valance electrons are largely bound in sp^3 hybridized covalent sigma-bonds. As a result of this bonding, the valence electrons have a very low mobility and are not able to significantly contribute to electrical conduction. Conjugated polymers however have a backbone of sp^2-hybridized bonds, which leaves one electron in the p^z-orbital, combining to a molecular wide set of dislocated wavefunctions [10, 13, 14, 15]. The mobility of these electrons is governed by their availability: when the polymer is 'doped' by oxidation, some of these delocalized electrons are removed and the material will conduct electricity. Undoped conjugated polymers on the other hand have a very low electrical conductivity (in the order of 10^{-8} to 10^{-10} S/cm). After doping of only a few per cent, electrical conductivity can rise up to 80 kS/cm in polyacetylene [6].

The most basic OLED design is a simple three-layer junction in which an electroluminescent polymer is sandwiched between two electrodes (see figure 1.1). Electrons are injected from a cathode into the π^*-antibonding orbital (corresponds to the lowest unoccupied molecular orbit, or the LUMO) of the polymer and holes are injected from an anode into π -bonding orbital (corresponds to the highest occupied molecular orbit, or HOMO) [11].

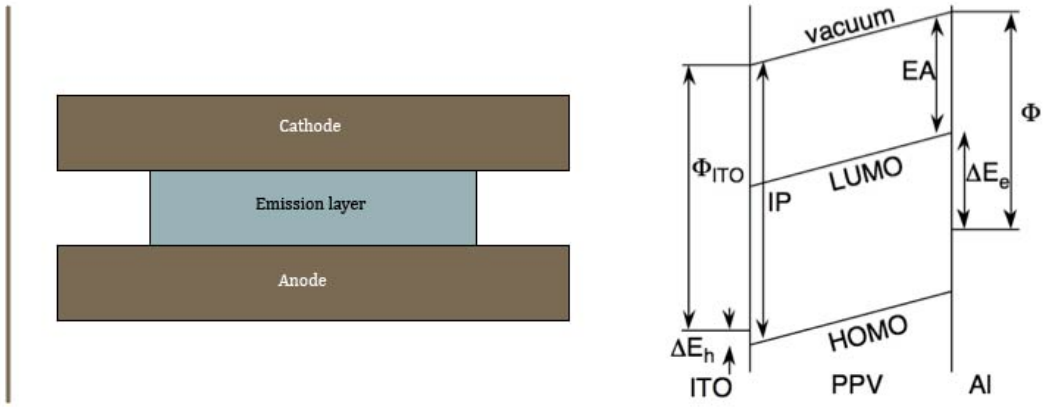

Figure 1.1: Device structure and bandstructure of a typical three-layer ITO-PPV-Al OLED. Φ_{ITO} and Φ_{Al} represent the work functions, E_h and E_e are the barriers to hole and electron injection and the IP and EA represent respectively the ionisation potential and electron affinity

Recombination

Inside the polymer, the injected holes and electrons travel from one side to the other, while on their way they can recombine by a variety of physical processes. These include multiphonon emission (non-radiative lattice vibrations assisted annihilation) or Auger recombination. The physics of these processes are not substantially different in organic materials from inorganic materials [11, 16]. When recombining, the electron-hole pair forms a neutral, strongly localized exciton. The eigenstate of the spin-wavefunction of this exciton can equal either S = 0, or S = 1, which corresponds to the so-called singlet and triplet states. Only the singlet state can produce spin-allowed radiative emission [17]. Quantum statistics dictates that one out of four excitons are formed as singlets: this limits the maximum quantum efficiency to 25%. However, electrons can cross-over from the singlet state to the triplet state and vise versa. The energy difference between these states (the exchange energy) governes the likeliness of this event to occur. A large energy difference corresponds to an unlikely cross-over, a small differences makes the process more probable [18, 19].
It is possible to make efficient use of the 75% triplet excitons, because they can contribute to light emission by indirect processes. This is done for instance by using heavy atoms with strong spin-orbit coupling for phosphorescence, or by triplet-triplet annihilation [9]. In order for the electrons and holes to recombine, they (or at least one of the species) must have a sufficiently low mobility so that local charge density can get high enough to find a recombination partner nearby. For more details on this, see [20].

The energy of the emitted photon equals the size of the band gap between the HOMO and LUMO levels of the chromophore. This is typically between the 1.4 and 3.3 eV, giving light with wavelengths between respectively 890 and 370 nanometre. By altering the morphology or position of the chromophore inside the polymer one can change the colour of the emitted light [16].

Charge injection

The interface between the electrodes and the emitting layer are of crucial importance for device performance. Charge injection in electroluminescent polymers is controlled by the energy difference between the work functions of the electrodes and by the electron affinity / ionization potential, for cathode / anode injection. Small energy differences correspond to smooth injection. There is growing evidence that unintended chemical reactions occurring on the electrode-polymer interface can form an insulating layer: the likeliness of this to happen depends mainly on the used materials and the cleanliness of the materials used [17]. Therefor, normally processing is done solely inside cleanrooms.

More advanced devices

So far only a simple three-layer setup of organic light emitting devices has been considered. This setup suits for evaluation of for example different electroluminescent polymers, but does not give optimal quantum efficiency. To avoid carriers from crossing the emitting layer without recombination, extra layers that can block or

facilitate specific kinds of charge transport are interspersed between the electrodes and the emitting layer (figure 1.2). An electron transport layer (ETL) is used to facilitate electron transport. This is done by growing a thin-film of a material with a higher valance band and a lower electron affinity than that of the emitting layer. The opposite counts for hole transport layers (HTL) [21, 22, 23]. For HTLs, p-doped conjugated polymers and metal oxides are often used [24]. Oxadiazole compounds are regularly used as an ETL [25]. For most applications, the anode contact of the organic light-emitting device is made from the transparent conductor Indium Tin Oxide (ITO). This is done to allow the light generated within the diode to leave the device. The cathode contact is usually metallic.

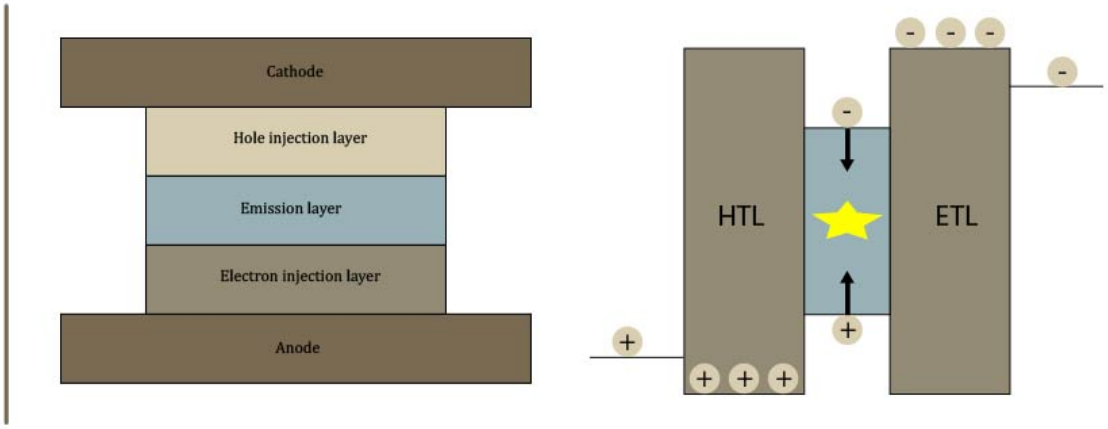

Figure 1.2: A Multilayer-setup OLED and its band diagram. Electrons are injected from the cathode and move through the electron injection layer. Holes are injected from the anode into the hole injection layer and they recombine inside the emission layer. Adding a HTL and a ETL improve the efficiency of the device

An intrinsic consequence of the processing of polymers in thin films is the possibility of unwanted electronic interactions between neighbouring chains. The degree of these interchain excitations can be controlled by varying the solvent or polymer concentration and has large consequences for the performance of the device [26].

1.3 | Experimental procedures and device testing

To grow the different layers inside the pores of nanoporous metals, most conventional growing procedures such as chemical vapour deposition or spincoating are not applicable. Previous work of E. Detsi and I. Gavrila suggests that the method of electrochemical polymerization / electrochemical deposition can be used to put thin coatings on the ligaments of nanoporous gold. The use of this method does give rise to a rather large constraint on the choice of materials, because only few can materials can be grown using these methods. Previous work of Chen et al. [27] suggests that a specific oxidation state of the conjugated polymer polyaniline (PAni) is electroluminescent and can be used as an emitting layer for the OLED. Literature also states that the polymer PEDOT:PSS suits well as a hole injection layer [28] [29] and metal oxide ZnO as an electron injection layer [30].

MK-group master student I. Gavrila already managed to make a semi-3D device consisting of one 3D contact between the nanoporous gold contact and the emitting layer of PAni (emeraldine base, see section 1.3.1 on page 12) and a 2D contact between the emitting and the hole injection layer (PAni emeraldine salt, see figure 1.3). Her device was tested at voltages ranging from -3V to 3V, up to -6V to 6V (figure 1.4). The I-V characteristics do not show any rectifying or non-linear diode action, but there is a significant photocurrent of 4 orders of magnitude. A corresponding movie to her thesis shows that the areas of ITO don't light up as a whole as expected, but that the light emission is very local.

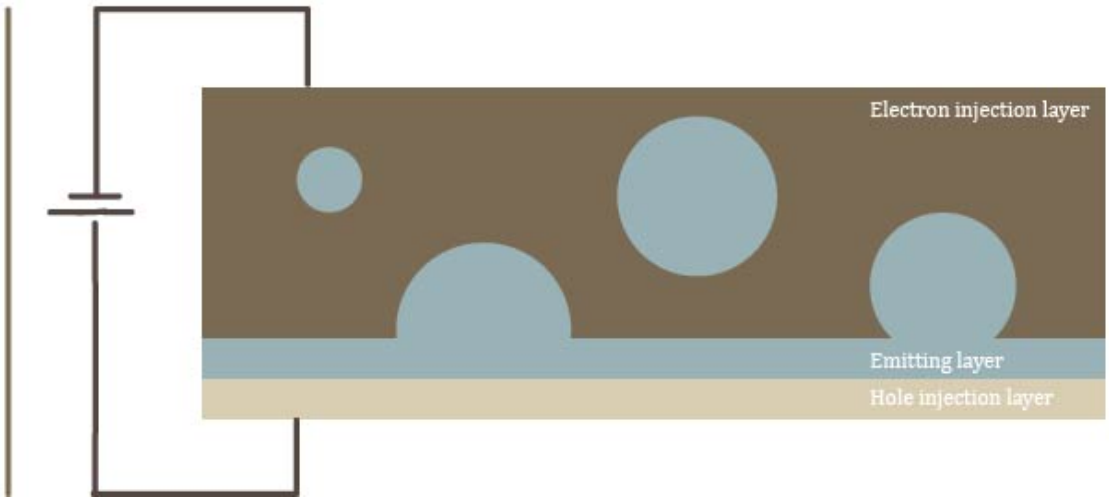

Figure 1.3: Semi-3D device with a 3D contact between electron injection and emitting layer and a 2D contact between the emitting and hole injection layer

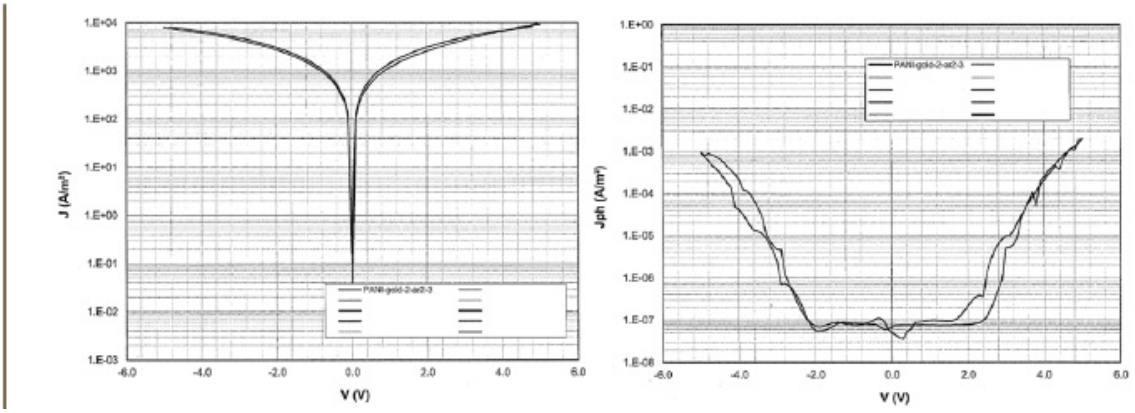

Figure 1.4: A plot of the I-V characteristics of the tested semi-3D device is shown on the left. It can be seen to be non-rectifying with its current approaching 10^4 A/m^2. As shown on the right, the OLED starts emitting light at -2 and 2 volts, reaching to a photocurrent of $10^{-}3$ A/m^2

1.3.1 Device design

Nanoporous gold (NPG)

Gold leafs consisting of 12 carat gold / silver alloys are dealloyed by leaving them to float in a bath of 65% concentrated nitric acid (Merck, Germany). Silver, as being the electrochemically most active constituent dissolves into the acid leaving a nearly pure gold leaf. Prior to the dealloying process no porous microstructure exists in the alloy. The pores form because the gold atoms are chemically driven to aggregate into clusters, resulting in a disordered porous network due to spinodal decomposition [1, 2]. After one hour all the silver is dissolved into the acid; the pore size can be governed by coarsening the gold leaf in an oven for a few hours. After heating the sample in nitric acid for 2 hours at 90 degrees Celsius a mean pore size of approximately 70 nanometres is obtained (figure 1.5).

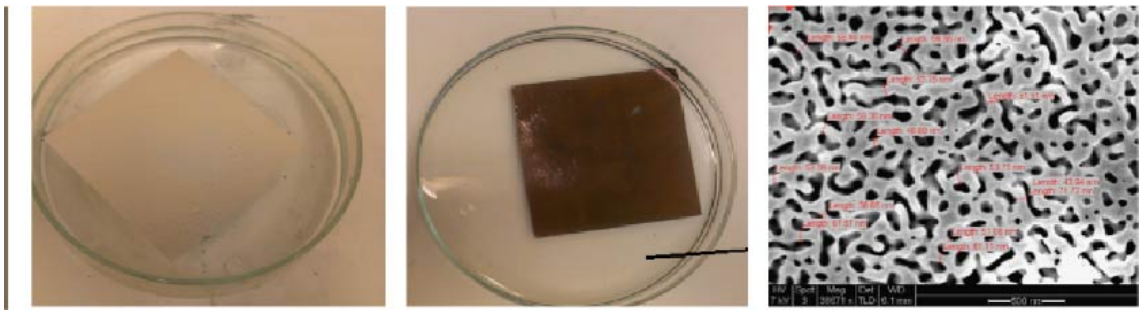

Figure 1.5: After dealloying, all silver atoms dissolve into the nitric acid and a nanoporous structure is formed (left and middle). The right picture shows an electromicrograph of the disordered porous structure of te NPG

Electrochemical polymerization

To grow thin polymeric films inside the pores of NPG, the method of electrochemical polymerization is utilized. A three-electrode cyclic voltammetry setup (figure 1.6) is used, with the monomer dissolved into the electrolyte. A working electrode (Au) is connected to the floating gold leaf, a Ag/AgCl reference electrode is placed in the electrolyte and the gold counter electrode lies underneath the sample. A triangular wave voltage is set over the reference and working electrode, which leads to monomer deposition on the working electrode. This is followed by electrochemical oxidative polymerization, due to the formation of radical cations at the monomers by electron transfer between the electrodes. Because the working electrode is connected to the nanoporous gold leaf, a polymer thin film grows onto the ligaments of the nanoporous gold. The resulting current at the working electrode is plotted against the applied potential to form a voltammogram as in figure 1.8.

Many electroluminescent conjugated polymers precursors dissolve fairly poor into organic and non-organic solvents. Sufficient diffusion of the monomers to the electrode surface is hard to reach without enough solubility of the precursors in the electrolyte. Under these circumstances, one must apply a relatively high potential, which inevitably leads to structural defects. This could affect the materials physical properties, such as its electroluminescence. Most polymers however will dissolve into solvents with high polarity and high dielectric constant such as acetonitrile.

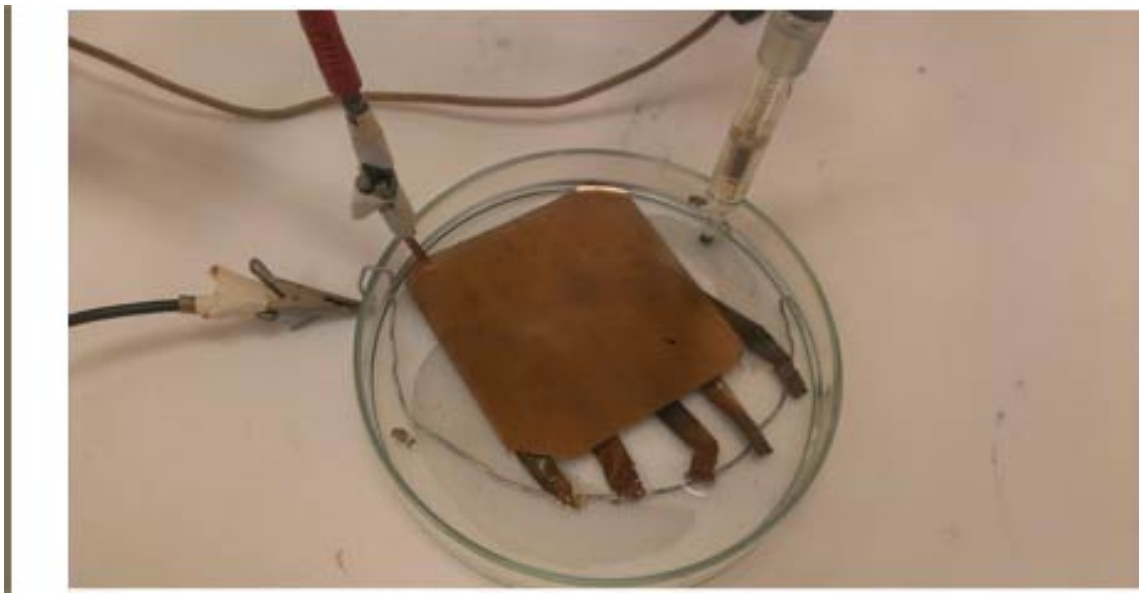

Figure 1.6: The three-electrode setup for electropolymerization. The working electrode is connected to the floating gold leaf, the counter electrode lies underneath the sample and a Ag/AgCl reference electrode is placed in the electrolyte

PANI

The electrochemical polymerization (EP) process of PAni consists of three steps: at first the aniline monomer oxidizes at the anode, forming aniline cation radicals. Next, aniline radicals couple by elimination of two protons and rearomatize. By this process the monomer form dimers, forming oligomers and ultimately polymers. For more information on the electrochemical polymerization of aniline, please refer to [32, 33, 34, 35]. PAni occurs in many different oxidation states and all transitions between these oxidation states are manifested by colour changes. The green emeraldine salt form is the only electrically conductive state. After EP from an acid electrolyte (H_2SO_4), the partially oxidized green emeraldine salt (ES) form is grown. The PAni ES is doped with H^+ ions and the HSO_4^- counter ions are inserted in the PAni matrix in order to maintain charge neutrallity. The PAni ES can be undoped to the blue emeraldine base (EB) by an alkali, or fully oxidized to the dark blue pernigraniline salt / base. The reduced state of PAni is called leucoemeraldine.
The fully oxidized and fully reduced states are poor conductors, even when they are (heavily) doped with an acid. The doped partially oxidized state however is highly conductive. This research focusses mainly on the emeraldine base state, for its supposed electroluminescent properties. See figure 1.7 for the chemical structure formulas of the different oxidation states.

The mechanism for electrical conduction of PAni was first investigated by Richter et al [36] and is somewhat different from most conducting polymers. Normally, a radical cation is formed at a carbon atom, whereas in the case of PAni radicals form at the nitrogen atoms involved in the conjugated double bonds. This means that the conductivity of PANI depends on both the oxidation state and the doping (protonation) level. The conductivity of PAni for the different oxidation states ranges from 10^{-2} S cm^{-1} to 10^{3} S cm^{-1}.

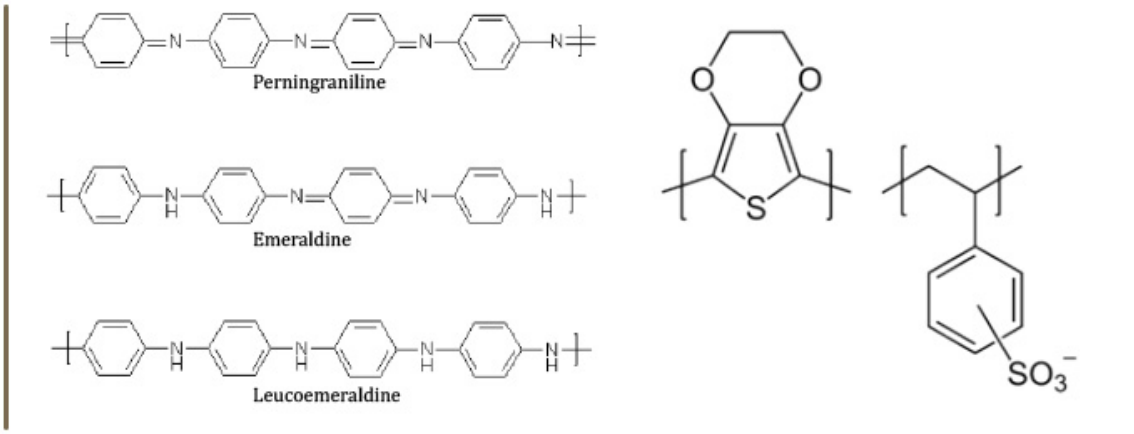

Figure 1.7: On the left the three oxidation states of PAni are shown. Pernigraniline is fully oxidized, emeraldine partially oxidized and leucoemeraldine is fully reduced. The structure formula of PEDOT:PSS is shown on the right

During the experiments, PAni (ES) was grown from a 0.5 M H_2SO_4 aqueous electrolyte with 50 mM aniline (Sigma-Aldrich, Germany). As seen in figure 1.8, oxidation peaks are found at 0.5 V and 1.1 V versus the Ag/AgCl reference electrode and the reduction peaks are around 0.3 V and -0.2 V. PAni grows autocatalytically, which makes the rate of polymerization increase as a thicker film is grown. The film was electrochemically deposited using cyclic voltammetry from -0.2 V to 1.1 V to -0.2 V with a scan rate of 50 mV/s and potentiostatically at 1.2 V vs. Ag/AgCL. The PAni was grown on the bottom of a NPG sample as well as on ITO substrates. The best results were obtained using cyclic voltammetry for about 10 cycles, resulting in a uniform green coating. After treatment with 0.5 M ammonium the green emeraldine salt is de-doped to the blue electroluminescent emeraldine base (see figure 1.8). Growing a PANI layer onto NPG resulted in a much more ductile gold leaf. Various attempts to grow the emeraldine base directly from an aqueous solution (added 0.2 M KCl to ensure sufficient conductivity) have failed.

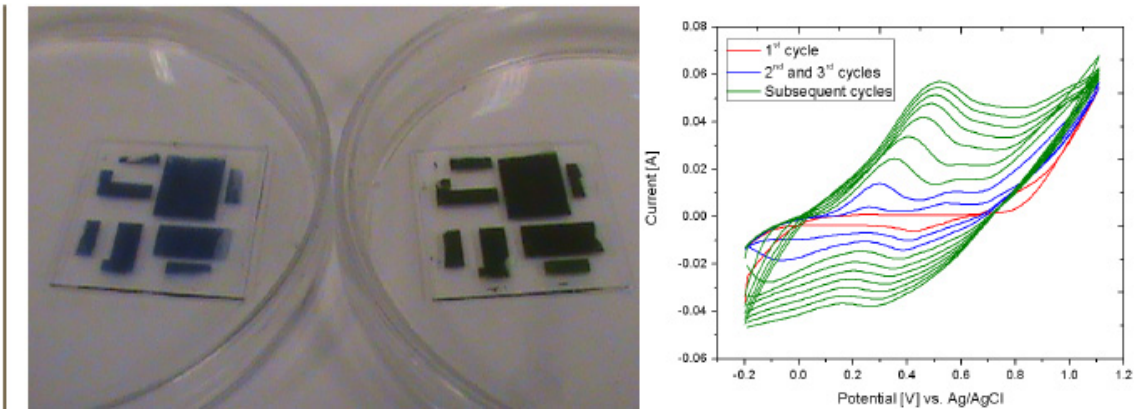

Figure 1.8: The blue electroluminescent emeraldine base is shown on the left and the emeraldine salt is pictured at the right. The graph shows the different oxidation states of PAni during the EP process at different potentials. [0] for the leucoemeraldine, [0,5] for the emeraldine salt / base and [1] for the fully oxidized perningraniline. The doping (protonation) results from binding of HSO_4^- ions to the aniline monomer

PEDOT:PSS

Another much used polymer for electropolymerization is poly(3,4-ethylenedioxythiophene) polystyrenesulfonate, or PEDOT:PSS (figure 1.7). PEDOT (like PAni) is a conductive conjugated polymer with interesting electrical properties, such as a low band gap (depending on its oxidation state between 1.4 and 2.5 eV) and high conductivity, which makes it suitable as a hole injection layer [37]. Its high light transmission and easy processability are also attractive features. The exact kinetics of the EDOT electropolymerization process are currently under investigation [38, 39, 40, 41], although there are some generally accepted mechanisms. The first step is the oxidation of the EDOT monomer, which diffuses towards the substrate-solution interface to begin oligomerization. When the surface becomes saturated with oligomers, a film begins to grow on the substrate forming specific areas, called growing nuclei. These regions expand to form the desired film. PEDOT can be produced with many different counterions, most notably PSS and LiClO4.

A drawback is that the monomer EDOT is insoluble in water; therefore PEDOT films are usually synthesized from organic solvents, such as acetonitrile. Our experiments have showed however that the acetonitrile destroyed (shrank) the nanoporous gold sample. This is probably due to the high dipole moment of the solvent, which makes molecules bulk up in the pores of the gold and destroy the sample from within due to large local attractive / repulsive forces. The used NPG foils are very thin (approximately 100 nm); if the NPG would have been thicker, this might not have happened. Please refer to the discussion section for more on this subject. The voltammogram that resulted from the electrochemical polymerization process of PEDOT:PSS is shown in figure 1.9

Electrochemical deposition of ZnO

ZnO layers have been grown electrochemically on ITO glasses from an aqueous 50 mM $Zn(NO_3)2*2H_2O$ (Alfa Aesar, UK), 0.5 M $NaNO_3$ (Merck, Germany) solution. The best films were deposited after cyclic voltammetry of approximately 4 cycles from -1.5 V to -0.2 V to -1.5 V with a scan rate of 50 mV/s. To ensure conductivity between the different zones of the ITO glass, the edges were manually covered with conducting silver paste (silver in methyl-iso-butylketon), as is seen in figure 1.10. ZnO is an n-type semiconductor with a bandgap of 3,4 eV and has a high exciton binding energy. The origin of the n-type behaviour of ZnO is a subject of discussion, but is commonly attributed to nonstoichiometry [42]. Another explanation lies in the presence of hydrogen impurities in the chrystal [43]. During the electrochemical deposition process a series of chemical reactions occur in the electrolyte and on the working electrode surface. Theses reactions as described by [44] are:

$$NO_3^- + H_2O + 2e^- \longrightarrow NO_2^- + 2OH^- \tag{1.1}$$

$$Zn^{2+} + 2OH^- \longrightarrow NO_2^- + Zn(OH)_2 \tag{1.2}$$

$$Zn(OH)_2 \longrightarrow ZnO + H_2O \tag{1.3}$$

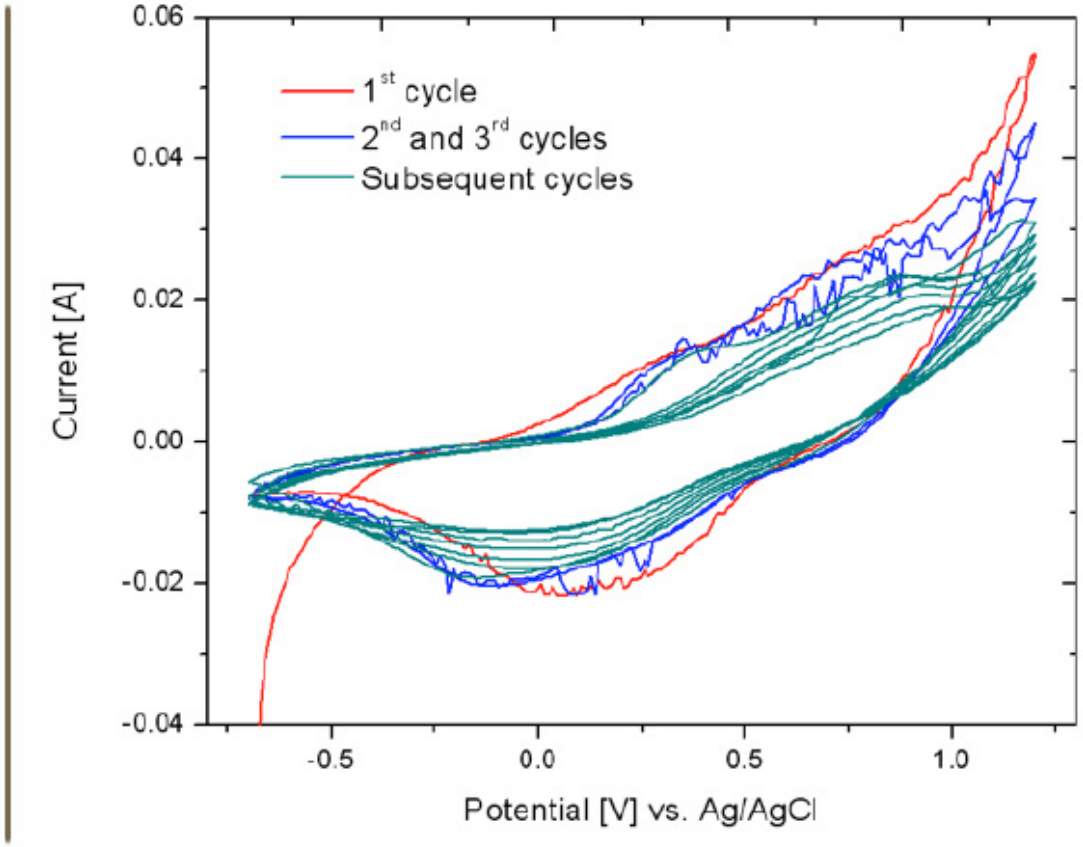

Figure 1.9: The voltammogram as obtained after growing PEDOT:PSS on an ITO substrate. The PEDOT:PSS was grown from 0.2 V to 1.2 V to 0.2 V, with a scan rate of 50 mV/s

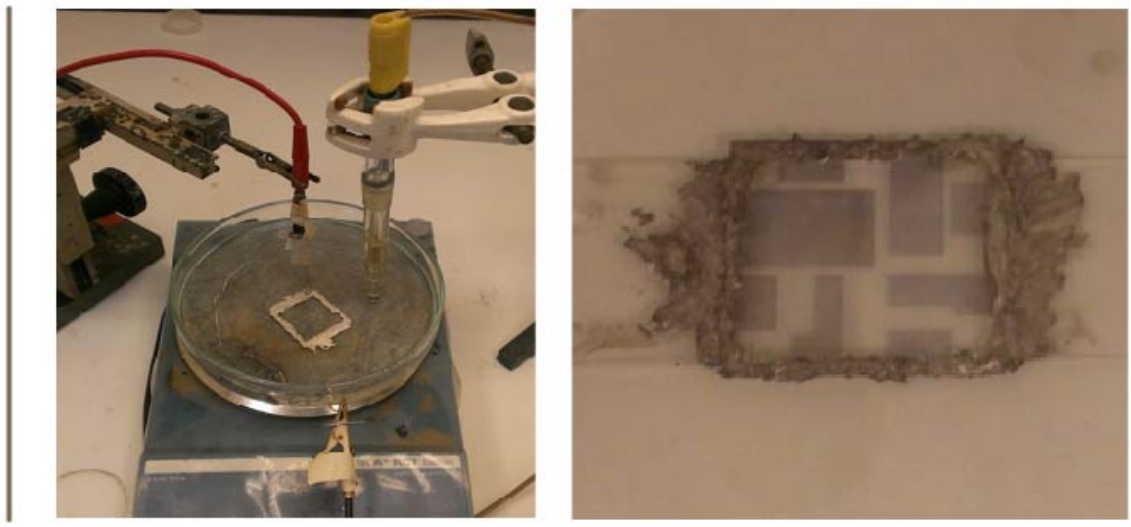

Figure 1.10: For electrochemical deposition on an ITO substrate, the edges of the sample were covered with silver paste to ensure enough conductivity. The ZnO coating is transparent white / purple

1.3.2 Device testing

Using the materials and techniques discussed in the previous sections, numerous devices with different junctions were made. An overview of the four devices with the most significant test results is given.

ITO-PEDOT:PSS-PAni (EB)-NPG

This sample was made by growing PAni (ES) in the pores of NPG and de-doping it to form the blue emeraldine base with ammonium. Next, a thin film of PEDOT:PSS was electrochemically grown onto the PAni (EB), so essentially a semi-3D device is made. In this sample NPG functions as both the anode and the electron injection layer. The hole injection is controlled by the PEDOT:PSS. The band diagram governing the carrier transportation is shown in figure 1.11. As stated in the experimental section, the acetonitrile used as a solvent for the PEDOT:PSS destroyed the NPG sample. However, after diluting the acetonitrile with water, the sample would still shrink, but not completely shatter. Measuring the I-V characteristics and photocurrent output shows some light output, but no rectification and a unusually high current of 10^4 A m^{-2}. PEDOT:PSS is a well studied material and known for its applications as a hole injection layer. However, for this purpose the acetonitrile solvent (even when diluted with water) leads to very difficult processing and makes PEDOT:PSS an unattractive HIL. Using PEDOT:PSS as the hole transport layer also leads to a large barrier for electron injection from the NPG to PANI (EB). Please refer to the discussion section for more on this subject.

Experiments concerning the fabrication of a fully operational 3D device prove to be hard to conduct due to the vulnerability of NPG, while the biggest challenges lie in determining the best fabrication conditions and the selection of materials. Therefore we decide to continue our work by first trying to make a 2D device and then extrapolating the results to the 3D configuration. To make sure that the results of the 2D device are also applicable to a future 3D device, all films are deposited by electrochemical deposition / polymerization.

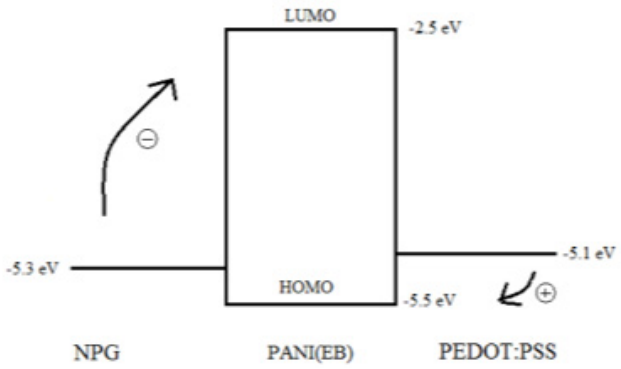

Figure 1.11: Electron and hole transport for the NPG-PANI(EB)-PEDOT:PSS junction. It can be seen that in this junction the barrier for electron injection is relatively high

ITO-ZnO-PAni (EB)-NPG

For this device, the green PAni (ES) was grown onto NPG and was then de-doped to blue PAni (EB). On the other hand, a layer of ZnO was electrodeposited onto an ITO glass and the ITO-ZnO glass was used to scoop a part of the floating NPG-PAni (EB). The band diagram of this device is shown in figure 1.12. While testing this sample, very small sections of the area's on the ITO glass lit up in an irragular fashion. A very high current was observed and the I-V diagram does not show any rectifying behaviour (as seen in figure 1.13). Therefore, it is most likely that the emitted light that was observed is caused by sparks and not by LED-action.

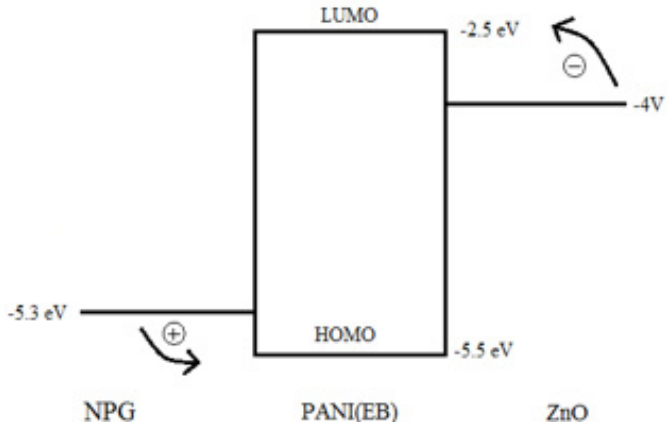

Figure 1.12: Due to the high work function of ZnO, efficient hole and electron transport layers are created by respectively NPG and ZnO

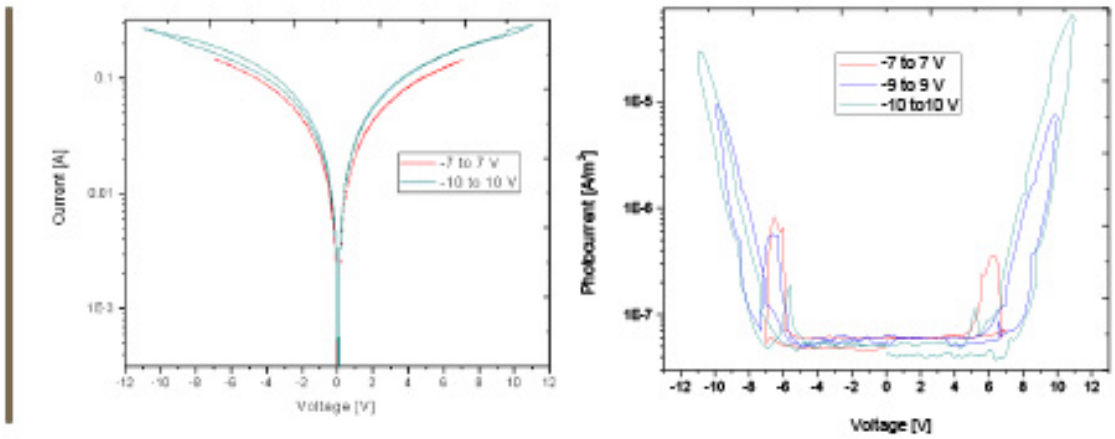

Figure 1.13: The ITO-ZnO-PAni (EB)-NPG junction shows a very high and non rectifying current. Therefore it is assumed that the light output is caused by sparks instead of regular LED-action

Reference device ITO–MoO_3–MEH:PPV–ZnO (VD)–Al

To be able to compare results, a reference device was made using cleanroom-techniques such as spincoating and vapour deposition. First, a layer of MoO_3 is spincoated on the ITO substrate, then layers of MEH:PPV, ZnO and Al are vapour deposited on

top of that. The MoO_3 provides for the hole transportation and the ZnO for the electron transportation as can bee seen in 1.14. ITO and Al serve as the contacts. MEH:PPV is one of the best studied organic luminescent polymers, which makes it an excellent luminescent material for a reference device. Upon testing, the device gave a very nice rectifying I-V characteristic and a large photocurrent, as seen in 1.15.

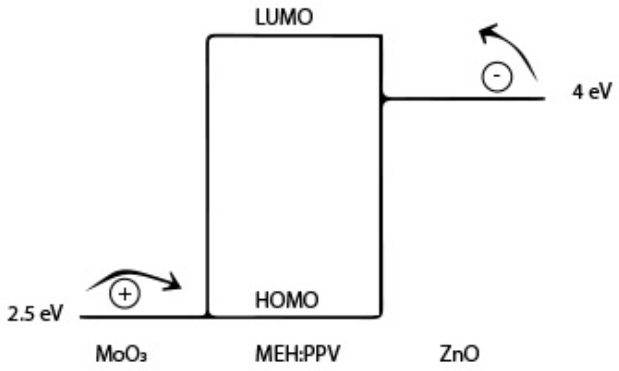

Figure 1.14: Vapour deposited MoO_3 takes care of the hole injection and spincoated ZnO the electron injection

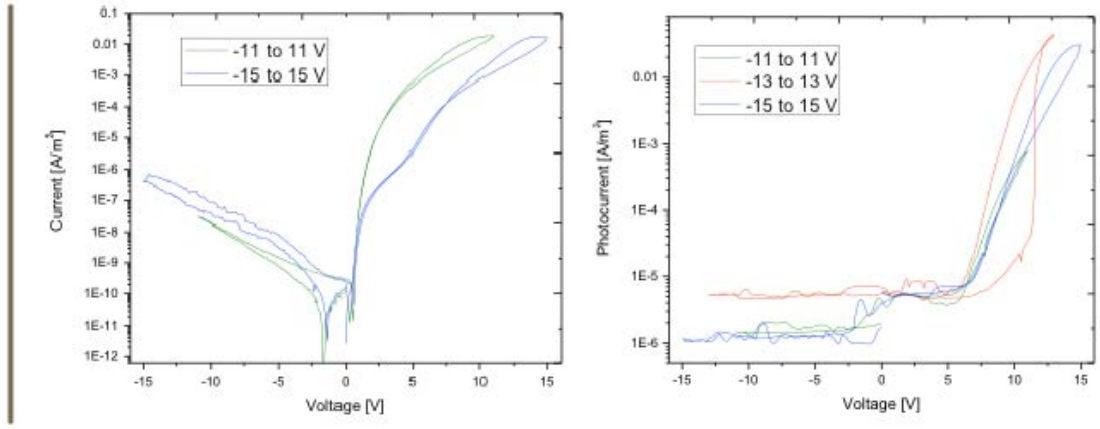

Figure 1.15: It is seen from the I-V diagram that the reference device has a distinct forward bias. At 15 V the forward current reaches up to 10^{-1} A/m^2 and the reverse bias current reaches 10^{-6} A/m^2. The photocurrent is measured being four orders of magnitude

ITO-MoO_3-MEH:PPV-ZnO (ED)-Al

Knowing the exact characteristics of a working OLED, a layer-by-layer analysis will provide insight in what went wrong with the ITO–ZnO-PAni (EB)–NPG junction. A sample is fabricated by electrodepositing ZnO on an ITO glass and again vapour depositing the MEH:PPV and Al contact, to see if the problem lies with the ZnO layer. The results shown in figure 1.16 show that although the ED of ZnO gravely disturbs the sample it still produces a significant photocurrent. This can be seen as a proof of concept for electrodeposition as a method of making OLEDs. Using ED does however lead to a large uncertainty in the fabrication process. Analyses of the layer thickness and surface roughness states that the grown layer is about a 100 nm thick and has a root-mean-square surface roughness of approximately 70 nm. This means that this layer could easily make short-circuits. Finetuning the experimental parameters could probably reduce the severity of this problem and thus produce cleaner results.

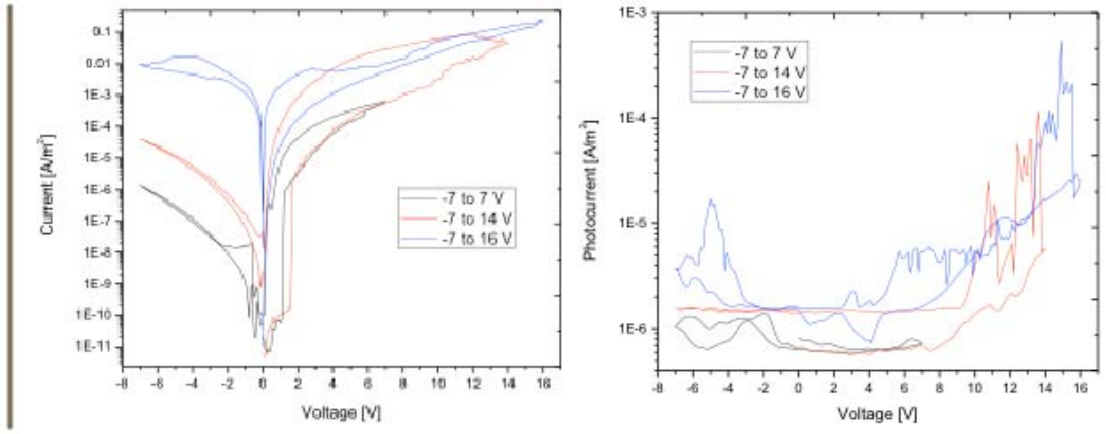

Figure 1.16: There it still a very clear forward bias in the I-V diagram and visible light emittance. The graphs however are gravely distrubed with respect to figure 1.15

Evaluation of PAni layer

Now it has been set that the ZnO layer cannot be the layer causing the failure of the ITO-ZnO-PAni(EB)-NPG device, the attention has turned to the PAni layer. A simple device was made by spincoating PAni (EB) directly from its solution and damping a barium HIL and an aluminium contact on top of it (both proven very effective in their kind). Careful analyses of multiple samples revealed no photocurrent at all. This gave rise to concerns on the electroluminescent property of PAni (EB), which were confirmed by checking a spincoated PAni (EB) film under ultraviolet light as seen in figure 1.17 and comparing it with the same device, using MEH:PPV instead of PAni (EB). No fluorescence at all was observed.

To make sure that it really was PAni (EB) of which the photoluminescence was measured, the optical absorption spectra of the spincoated liquid has been measured: figure 1.18). We measured peaks at 420 nm and 900 nm for the emeraldine base and one broad peak at 550 nm for the emeraldine salt. This is reasonably consistent with previous work of I. Gavrila, who measured two peaks at 480 nm and 850 nm

for the EB and two close peaks between 450 nm and 650 nm for the ES. The shift in peaks can be explained by the fact that the measurements were made with different solutions.

Other literature shows that the optical absorption peaks for PAni EB lie at 550 nm and 850 nm and that PAni ES has a broad peak around 780 nm and a smaller one at 343 nm [45]. Although the lower peak cannot be found in our results, nor in I. Gavrila's, it can be stated that our results are consistent with the results shown in previous work.

To make sure that the spincoated PAni EB layer is reasonably smooth, the surface roughness is evaluated using a Taylor Hobson Form TalySurf PGI 840. The measurements were conducted by people from Sumipro Submicron Lathing BV. The surface roughness is indicated by two key parameters, the peak-to-valley distance and the root mean square surface roughness. The measurements show that the PAni EB layer is smooth with a RMS of 3.7 nm. The peak to valley measurement indicates a spread of 56 nm, indicating the presence of local contamination of some sort. However, overall it can be stated that the spincoated PAni EB layer is of good quality. The measurement results of the surface roughness of PAni EB, together with that of untreated ITO-glass, can be found in appendix A on page 32

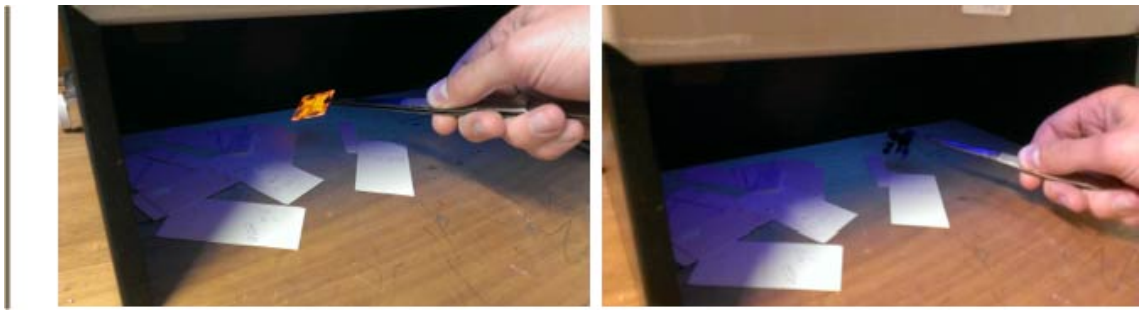

Figure 1.17: On the left the fluorescent property of MEH:PPV is demonstrated under a source of UV-light. To the right a sample with spincoated PANI (EB) is shown, which gives no fluorescence

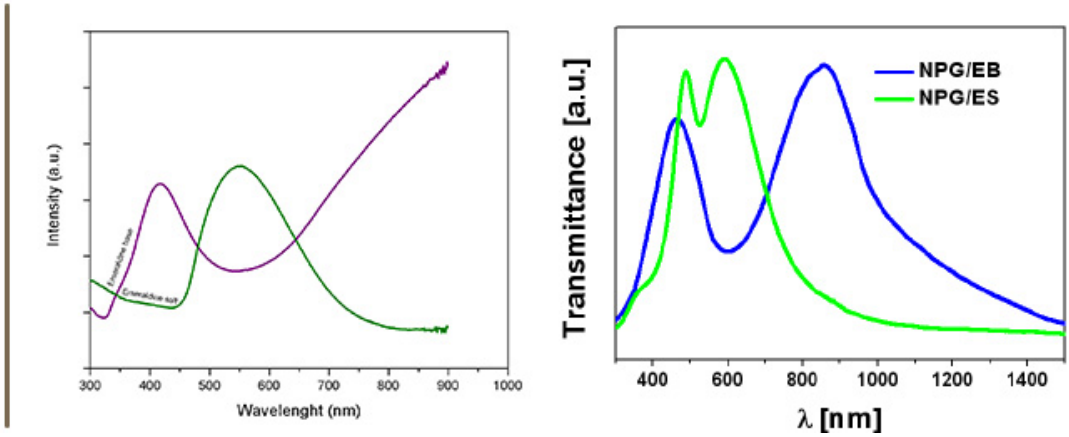

Figure 1.18: On the left our own measurements of the spectrum of PAni EB is shown. It is seen that the figure closely resembles the results as obtained by I. Gavrila, as is shown in the right graph

1.4 | Discussion and suggestions for future work

Why PANI (EB) does not work as an emitting layer

In spite of the results that Chen et. al. published in 1996 in their paper "White-light emission from electroluminescence diode with polyaniline as the emitting layer" [27], we have found no light emittance of devices in which PAni EB was used as an emitting layer. Also no rectifying I-V characteristics and even no photoluminescence was observed from spincoated PAni EB. There are several possibilities for why PAni EB did not emit light. First of all, the different oxidation and doping states of PAni have very distinct specifications. We have found that is was very hard (or maybe even impossible) to grow PAni EB directly from water, so our method of growing the emeraldine base was first growing the green emeraldine salt from an acid solution and then doping it with ammonium to the emeraldine base. It is possible that during the growing or the doping process, the PAni oxidized and perningraniline base was obtained instead of emeraldine base. However, analyses of the uv/vis absorbtion spectra showed that the grown material was indeed PAni EB. Therefore, the most probable conclusion is that PAni EB is in itself not electroluminescent and thus is unsuitable for use as an emitting layer in OLEDs.

Fine-tuning the ZnO / PEDOT:PSS hole injection layer

The PEDOT:PSS hole injection layer did show some light output, but did this at a very high current (10^4 A) and without any signs of a rectifying I-V characteristic. Most probably the light emittance is caused by short-circuits, rather then by genuine LED action, for this would explain the linear behaviour and high current. As discussed, PEDOT:PSS only dissolves in highly polar solvents such as acetonitrile, which causes massive damage to the nanoporous sample. Diluting the PEDOT:PSS with water reduces the damage, but does not prevent the damage completely. Although optimisation could probably come a long way in minimizing this problem, I would discourage future work on this area, because other hole injection layers are much easier to process. Other materials are also more energetically favourable because the HOMO / LUMO levels of NPG and PEDOT:PSS lie very close to each other (respectively 5.3 and 5.1 eV), which makes the electron injection less efficient then for example with ZnO.

Devices made with a electrochemically grown ZnO hole injection layer did produce light and a rectifying I-V characteristic, but did that at a grave loss of efficiency. This is most probably due to the high surface roughness and the spongy structure of the grown layer. However the results serve as a prove of concept that ZnO is suitable to be used for this purpose, future research must clarify the specific experimental conditions to make a high quality film. Probably diluting the zinc nitrate solution so that the number of cycles can be increased will suffice.

Alternatives for PAni (EB) as an emitting layer

So far we were unable to make use of electrochemically grown PAni (EB) as a suitable emitting layer for the 3D LED. However, a literature review of electrolumi-

nescent polymers shows that there are alternatives worth examining more closely. The properties a polymer should posses for our purpose is that it must be electrically conductive and electroluminescent. It must also be able to electrochemically polymerize from a monomeric solution to form a thin film on the nanoscale ligaments of nanoporous gold.

Two specific polymers seem to be suitable for our cause. There is proof that TCPC [46] and PFCzPO [47] are both electroluminescent and prepared by in situ electrochemical polymerization. The films prepared under optimized conditions show high fluorescence, smooth surface morphology and high OLED performance. As reported earlier, the quality of an electrodeposited polymeric film is largely dependent on its solubility in the electrolyte. Both TCPC and PFCzPO dissolve very well (up to 1 mg L^{-}1) in acetonitrile. PFCzPO has a highly fluorescent backbone (polyfluorene) with carbazole and phosphonate groups. The carbazol groups have a relatively low oxidation potential that leads to very efficient coupling between carbazol groups. Therefore, the polymer gets cross-linked which gives extra control over its structure. The phosphonate group has a high polarity that increases the polymers solubility in polar solvents. Another attractive property of the phosphonate groups is that it has efficient electron injection properties [48, 49].

Growing PFCzPO using cyclic voltammetry from 0 V to 1.2 V to 0 V a high quality film forms with a speed of approximately 2,5 nm per cycle at a scan rate of 400 mV s^{-}1. After growing a layer of 200 nanometres, a RMS surface roughness of ¡ 4 nm is reported. A single layer ITO/PFCzPO/Al device shows major photoluminescence from a turn-on voltage of 5.5 V.

It seems that PFCzPO (and in a lesser degree TCPC) are ideal candidates to replace PAni EB as the emitting layer in the 3D LED setup. There is however one major drawback: both polymers dissolve only in highly polar solvents such as acetonitrile, while acetonitrile destroyed the sample of nanoporous gold. Further experiments must show if this problem can be solved. We have already shown that a mixture of acetonitrile and water (50/50) only damages the sample, but not completely destroys it. One can also try using a bulk of nanoporous gold instead of a small lightweight leaf, since the bulk might be able to resist the attractive and repulsive forces resulting from the polar solvent. Other nanoporous metals then gold are also worth investigating, for they are cheaper to work with when using bulk materials.

Alternative methods for electrochemical deposition / polymerization

Many of the difficulties in the experiments are directly linked to the method of electrodeposition / polymerization. Although these methods give excellent control over film thickness, they severely limits the number of materials that one can use. The exact chemistry of polymerization process is often unclear and in-situ measurements of for example layer thickness is impossible. Unfortunately, more conventional deposition techniques as vacuum deposition or spincoating do not suffice in our case, since the surface that needs to be treated is not a 2D-surface, but a 3D gyroidal surface. The used technique must also allow different layers to be grown on top of

each other and have a RMS surface roughness order of nanometres.

Recent work of the group of Weismüller at the Technische Univerität Hamburg-Harburg [50] demonstrated that vacuum impregnation can be used to deposit polymers into the pores of nanoporous gold. In their case, this was done to improve the plasticity of the NPG, for which the thickness of the coating makes little difference. Using an epoxy resin and an amine hardener, the material is deposited by putting it in a vacuum chamber together with the NPG and as the vessel is vented, the liquid is pushed into the pores and any excess material is scraped off. This method gives no control over the layer thickness and fills all pores completely. That makes this deposition method suitable for a semi-3D device, but does not allow the deposition of different films in the pores, which is essential for the 3D device.

Another technology that might suit our application is that of ionically self-assembled monolayers (ISAM) deposition. ISAM films are formed by depositing alternately charged polymers from a solution onto the substrate. Coulombic attraction between the substrate surface and the polymer in solution results in a bonding of the polymer to the substrate. The reversal of surface charge limits the deposition of polymers to a monolayer, as the polymer solution is now repelled from the substrate. After taking out the substrate and cleaning it, another monolayer can be deposited by placing it in a second, oppositely charged solution. This process may be repeated indefinitely, until a layer of the desired size is obtained. The ISAM method is a good candidate for replacing electrodeposition / polymerization, for it gives good control over the film thickness and minimum surface roughness. It is also probably capable to penatrate into the 3D cavities of nanoporous gold. A possible drawback is that there is no polymerization, for a solution of polymers is used. Depending on the degree of polymerization and the pore size of the NPG, the polymers might not be able to penetrate into the material. ISAM deposition has already been successfully used for PLED and photovoltaic applications [51, 52, 53] using PPV and other thiophene derivatives. RUG professor Chieci from the group of Chemistry of Bioorganic Materials and Devices has published extensively on the subject of ISAM deposition.

Other popular deposition techniques such as molecular beam epitaxy, atomic layer deposition, sputtering or electrohydronamic deposition all have major issues for our application, mostly in the selection of suitable materials or in the geometry of nanoporous materials.

1.5 | Conclusions chapter 1

Extensive experimenting has shown evidence that PAni EB is not suitable to be used as an emitting layer for a light emitting device. Fortunately, there are other polymers that may very well suit our application, such as TCPC and PFCzPO. These polymers only solve in highly polar solvents such as acetonitrile and experiments have shown that this severely damages the NPG film. However, under the right experimental conditions the damage done to the NPG sample will probably be controllable. Zinc Oxide shows to be a suitable electron injection layer for our application and is compatible with electrochemical growth. This means a semi-3D device can be made consisting of ITO-ZnO-PFCzPO-NPG. Once finished, these results can be extrapolated to a fully operational 3D device by fine-tuning the layer thickness of ZnO and PFCzPO. Many of the problems encountered arose due to the unorthodox nanodevice fabrication mechanism of electrochemical deposition and polymerization. Future experiments must show if the polymers used for Ionically Self-Assambled Monolayers (ISAM) can penetrate into the NPG deep enough, for this can potentially solve some of the problems encountered while using electrochemical polymerization.

Chapter 2

Synthesis of silver nanoparticles

2.1 | Motivation

In Scanning Electron Microscopy (SEM) pictures, the surface topography is represented by contrast variations. Work conducted in the MK-group [54] (to be published) presents a new approach to obtain reliable surface reconstructions from 2D SEM images, by comparing images made at different microscope tilts using digital image correlation. An advantage of this method is that accurate 3D information is presented without difficult calibration algorithms that may introduce errors [55]. The method works even without requiring information on the tilt of the presented images. Our task is to calibrate and test the new software by making nanoparticles with a distinct shape and making electronmicrographs from it. To get maximum spread in contrast, the nanoparticles are grown onto nanoporous gold.

2.2 | Methods

Two completely different growing procedures proved to be suitable to synthesize the silver nanoparticles. There is no specific form configuration required, so tests were conducted with a range of different morphologies.

Polyol synthesis

Silver nanoparticles are often synthesized via the polyol process [56, 57] because of the low-cost experimental setup and flexibility in the growing process. Traditionally the formation of metal nanoparticles is a harsh process, because on a nanoscale metals tend to nucleate quickly in order to reduce their surface energy. By adding polymers as capping agent however, the reaction is influenced and morphologies with less stable facets can be formed. Here we report on the synthesis of silver nanoparticles by using ethylene glycol as both the solvent as the reducing agent of silver ions obtained from silver nitrate ($AgNO_3$). Polyvinyl pyrrolidone (PVP) is added as the capping agent. Depending on experimental conditions such as temperature, concentration and molar ratio between $AgNO_3$ and PVP, morphologies varying from cubes, to wires and spheres can be formed [58, 59]. The fundamental basis of the formation of the different shapes is yet to be fully understood, but it is believed that the selective absorption of PVP on various crystallographic planes of silver plays a major role [60].

Electrochemical deposition

The second method of synthesizing the silver nanoparticles is by electrochemical deposition. The theoretical background of this process equals that of the electrochemical deposition as describes in section 1.3.1 on page 14. Lower concentrations are used however to ensure slower particle growth.

2.3 | Experiments and Results

Polyol synthesis

The chemicals used are PVP with a weight average molecular weight of 24000 g mol^{-1}, $AgNO_3$ and ethylene glycol (EG), which are both bought from Sigma-Aldrich. Literature describes two experimental methods within the polyol process for making silver nanoparticles: heating the precursor and then adding it to the solution or precursor injection at a fixed rate. After trying both methods, the best results were found using the precursor injection method, resulting in silver nanospheres with an average diameter of approximately 15 nanometres (figure 2.1). This was done by heating 5 ml EG to 160 C° and carefully injecting 3 ml 0.6 M PVP and 3 ml 0.3 M $AgNO_3$ while vigorously stirring. It was found that the process depends very strongly on the temperature and the molar ratio between $AgNO_3$ and PVP. In this case the molar ratio ($AgNO_3$:PVP) equals 2. An experimental difficulty was that the used heating plate had an uncertainty in its temperature of ±15 C°.

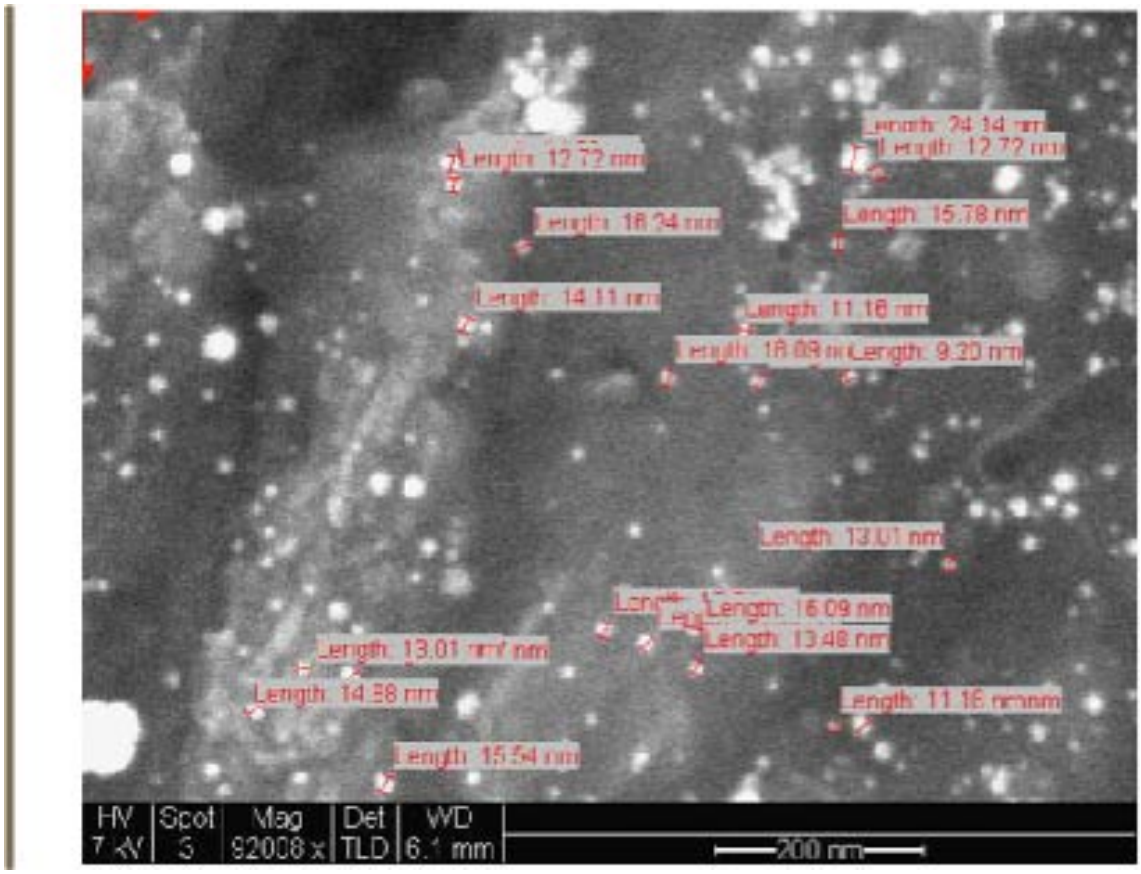

Figure 2.1: Uniform distribution of silver nanospheres with an average diameter of approximately 15 nm

At the same temperature, but with a $AgNO_3$:PVP molar ratio of 1.5, nanoparticles with a completely different shape were made. As shown in figure 2.2 silver nanocubes with an average diameter of 150 nanometres were synthesized. There is contamination of silver nanoparticles of other sizes and morphologies present, such as nanowires, spheres and pyramids.

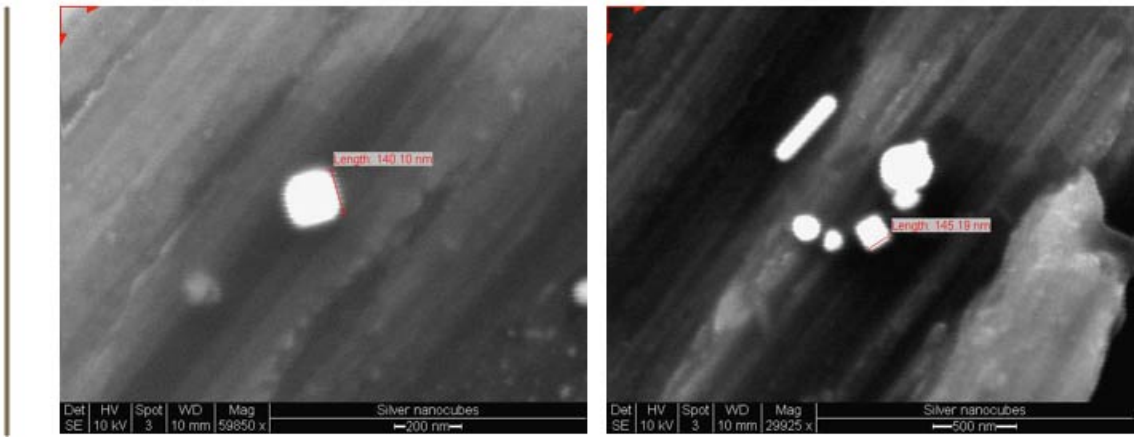

Figure 2.2: With a molar ratio between $AgNO_3$:PVP of 1.5, silver nanocubes are formed with a diameter of approximately 150 nm, among many other, more exotic structures

Electrodeposition

The experimental method used for the electrodeposition much resembles the procedure as described in section 1.3.1 on page 14. This time however a nanoporous gold leaf is used as the cathode, which has been coarsened in a furnace for one hour at 300 C° in order to increase the size of the ligaments. A silver foil is used as the anode and the electrolyte consists of 50 mM aqueous $AgNO_3$. A standard 3-electrode setup is used, giving a cyclic triangular current from -50 mV to +50 mV with a scanrate of 1000 mA/s and a step current of 1 mA. The resulting nanostructures are shown in figure 2.3. Large silver pyramids are observed with on the facets smaller silver particles. The ligaments of the nanoporous gold give a great contrast with the particles. When the images are observed with a dual beam microscope even smaller silver nanostructures are observed inside the pores of the NPG.

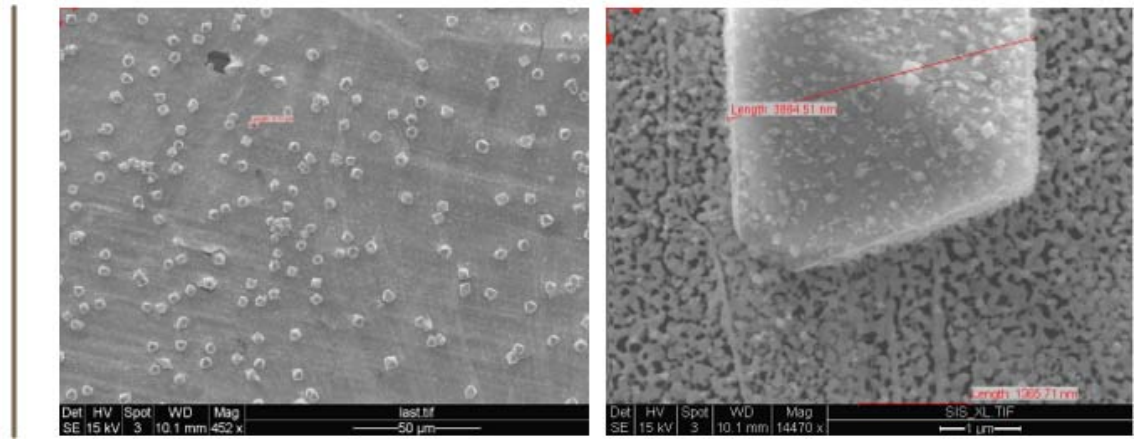

Figure 2.3: The electrodeposition of silver nanoparticles leads to a uniform distribution of large (3-4 micrometers) silver pyramids. Also notice the nanostructures on the facets of the pyramid.

2.4 | Discussion

Experiments have shown that both the polyol synthesis and electrodeposition are suitable for making silver nanoparticles. The experimental conditions of the polyol process are very stringent and many experiments were conducted before the right parameters have been found. The resulting silver nanoparticles were almost flawless, but alongside the nanocubes (molar ratio $AgNO_3$:PVP of 1.5) also many other unwanted morphologies were made. Therefore, although more unconventional, the growing procedure based on electrodeposition proved to be more convenient. Despite the fact that this method gives less control over the morphology, the experiments are easier and better reproducible. For the application of testing and calibrating the 3D imaging technique, the presence of little structures on the facets of the pyramids were also a nice feature. In the appendix SEM and FIB pictures are found made at angles varying from 0 to 12 degrees. These pictures served as input for the digital image correlation software. The software was able to produce the 3D image as presented in figure 2.4.

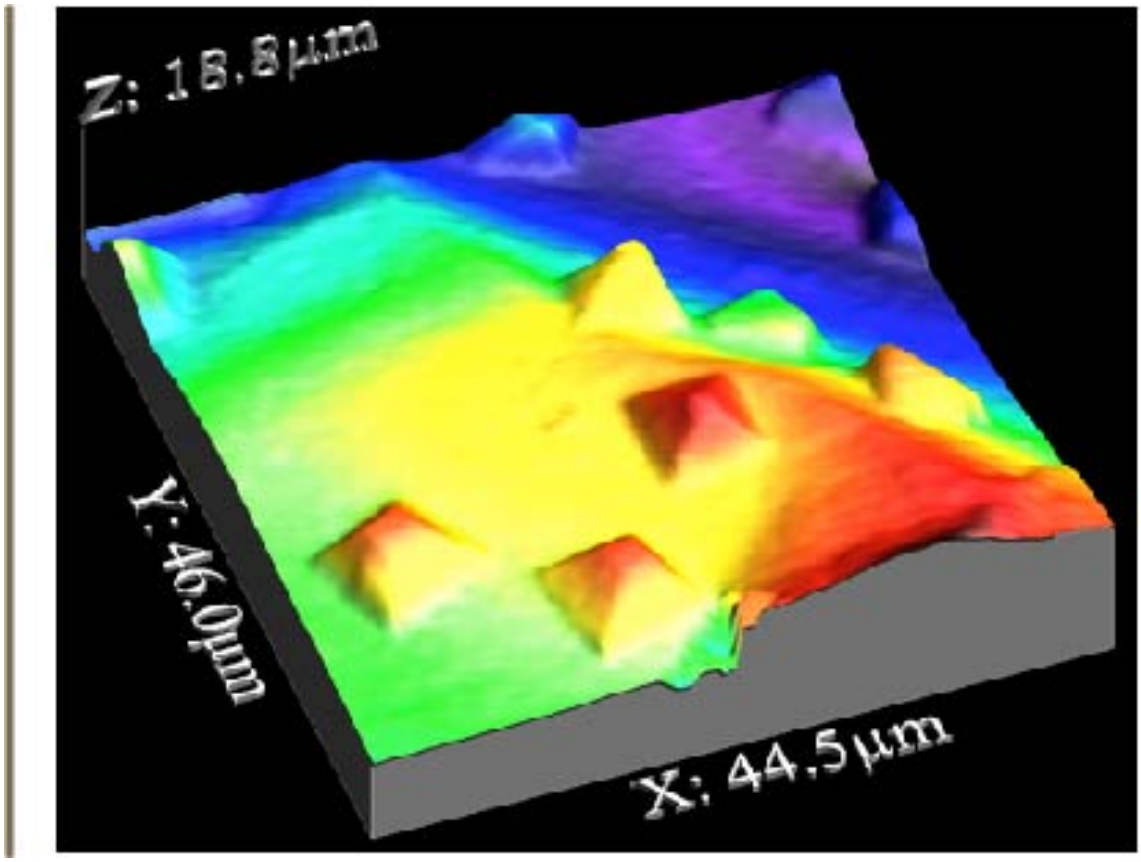

Figure 2.4: Novel digital imaging software made a 3D image from 2D electronmicrographs at different angles

2.5 | Conclusions chapter 2

Using both electrochemical deposition and polyol synthesis, it has been shown that both methods are suitable for making silver nanoparticles. Although the polyol method provides more control over the morphology, the electrodeposition technique gives cleaner en better reproducible results. Electron micrographs at angles between 0 and 12 degrees from the obtained pyramids on the NPG film have been successfully used in order to calibrate the novel software for which the patent is currently pending.

Acknowledgments

The last few months I have finally learned what it means to be an actual researcher. Under the sublime guidance of Eric, prof. De Hosson and the other group members I have found my time in the MK-group very inspiring and instructive. Special thanks goes to the group members of Physics of Organic Semiconductors and the professionals at Sumipro BV for their guidance and help during the experimental phase. Most experiments described in this thesis were conducted together with bachelor student Rick Meijerink, which whom I have colleborated extensively. I have admired your diligence and enjoyed our collaboration.

MK-Group
Prof. Dr. J. Th. M. De Hosson
Eric Detsi
Mikhail Dutka
Enne Faber
Rick Meijering
All other group members

Physics of organic semiconductors
Prof. Dr. L. J. A. Koster
Niels van der Kaap
Gert-Jan Wetzelaer
Jan Harkema

Sumipro Submicron Lathing BV
Gerald Hemel
Gert-Jan Waaiman

Appendix A

Surface roughness measurements

The surface roughness measurement as conducted by Sumipro BV of the spincoated PAni EB film.

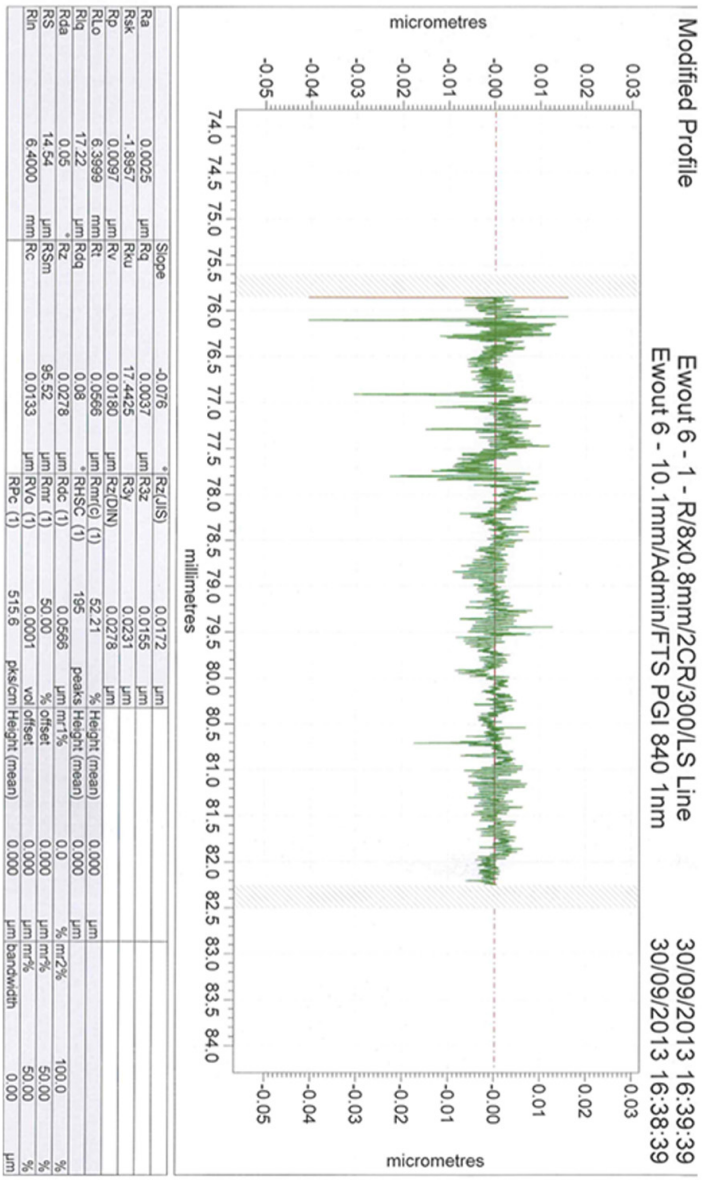

Figure A.1

The surface roughness measurement as conducted by Sumipro BV of untreated ITO glass.

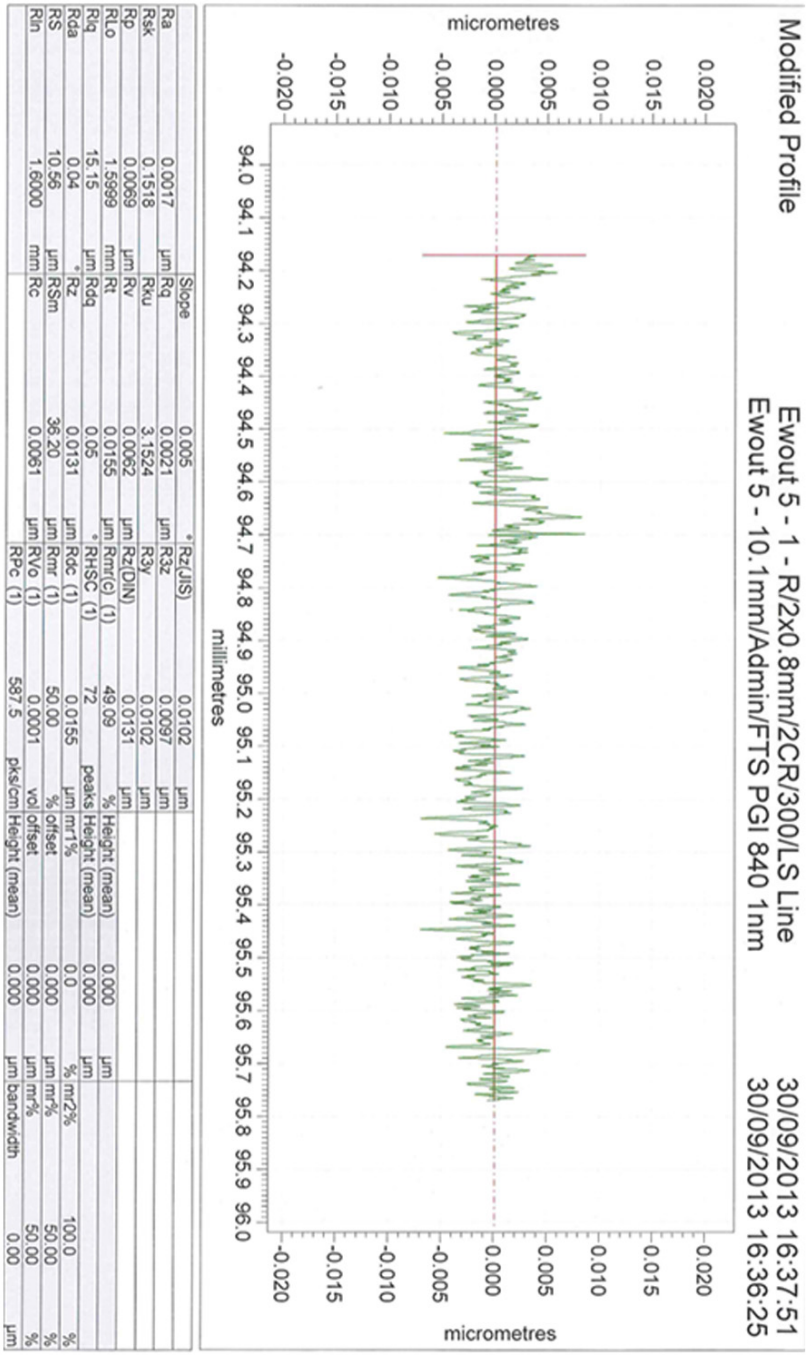

Figure A.2

Appendix B

Electronmicrographs nanoparticles

Electronmicrographs of silver pyramids taken with a Focussed Ion Beam. The pictures are taken at angles varying from 0 to 12 degrees.

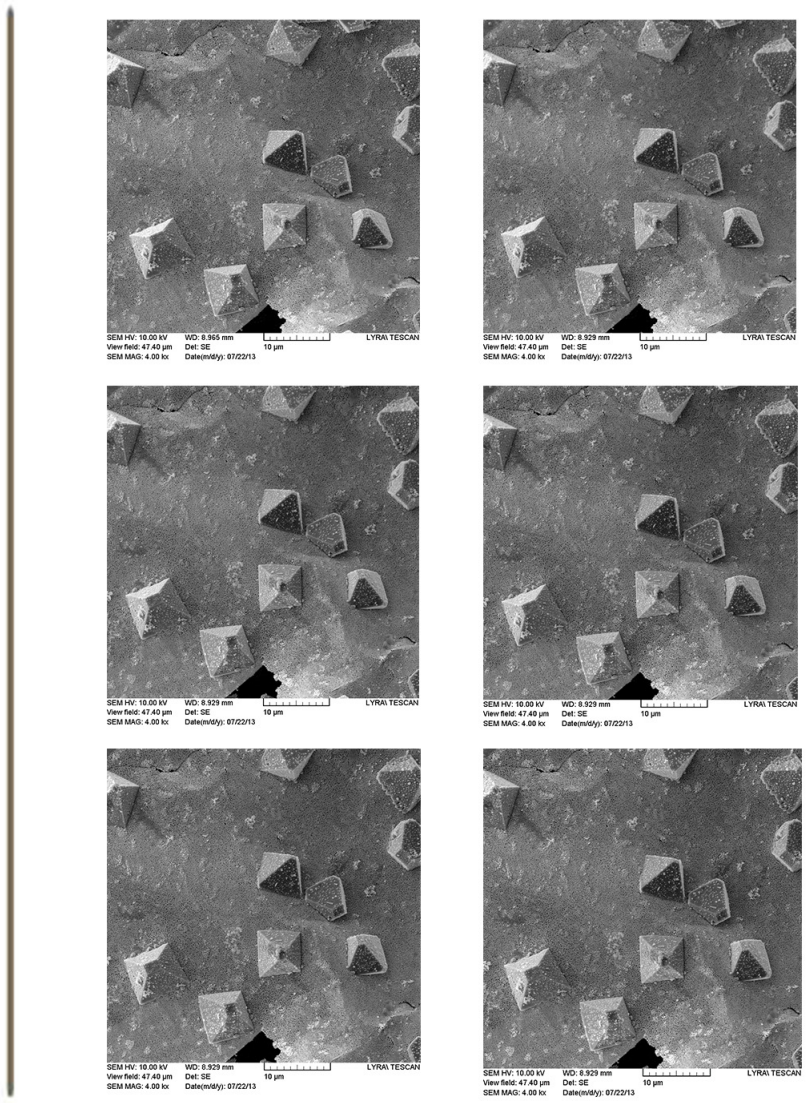

Figure B.1

Electronmicrographs of silver pyramids taken with a Environmental Scanning Elecronmicroscope. The pictures are taken at angles varying from 0 to 12 degrees.

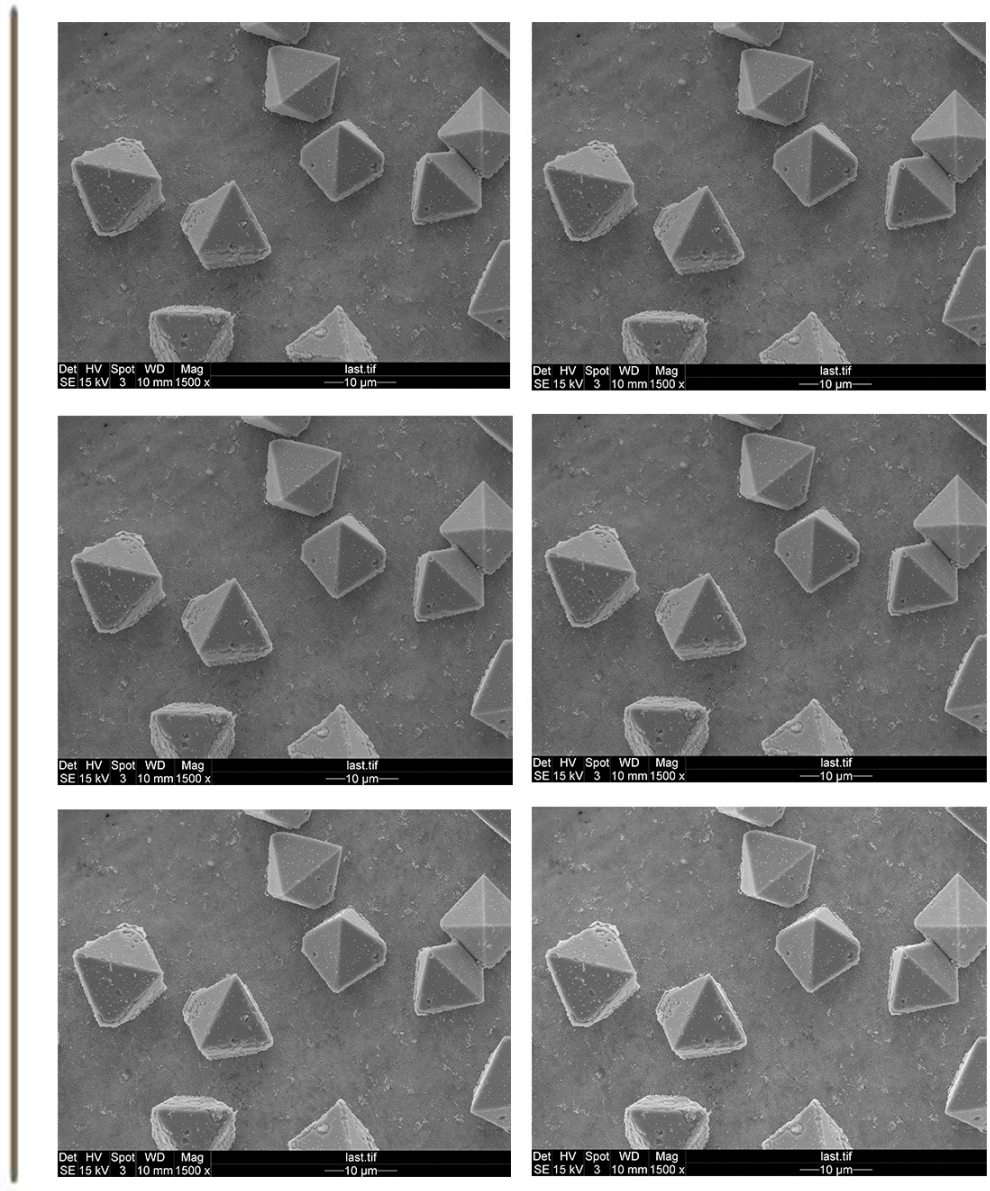

Figure B.2

Bibliography

[1] Karl Erlebacher, Jonah Aziz, Michael J.Karma, Alain Dimitrov, and Nikolay Sieradzki. Evolution of nanoporosity in dealloying. *Nature*, 410(6827):450, 03/22 2001. M3: Article.

[2] E. Detsi, E. De Jong, A. Zinchenko, Z. Vukovic, I. Vukovic, S. Punzhin, K. Loos, G. ten Brinke, H. A. De Raedt, P. R. Onck, and J. T. M. De Hosson. On the specific surface area of nanoporous materials. *Acta Materialia*, 59(20):7488–7497, DEC 2011.

[3] Ke Wang and Jörg Weissmüller. Composites of nanoporous gold and polymer. *Advanced Materials*, 25(9):1280–1284, 2013.

[4] E. Detsi, P. R. Onck, and J. Th M. De Hosson. Electrochemical artificial muscles based on nanoporous metal-polymer composites, 2013.

[5] E. Detsi, P. R. Onck, and J. Th M. De Hosson. Metallic muscles at work: High rate actuation in nanoporous gold/polyaniline composites. *ACS Nano*, (5):4299.

[6] C. K. Chiang, C. R. Fincher, Y. W. Park, A. J. Heeger, H. Shirakawa, E. J. Louis, S. C. Gau, and Alan G. MacDiarmid. Electrical conductivity in doped polyacetylene. *Phys. Rev. Lett.*, 39:1098–1101, Oct 1977.

[7] Alan J. Heeger. Nobel lecture: Semiconducting and metallic polymers: The fourth generation of polymeric materials. *Rev. Mod. Phys.*, 73:681–700, Sep 2001.

[8] J.H. Burroughes, D.D.C. Bradley, A.R. Brown, R.N. Marks, and K. Mackay. Light-emitting diodes based on conjugated polymers. *Nature*, 347:539–541, October 1990.

[9] Bernard Geffroy, Philippe le Roy, and Christophe Prat. Organic light-emitting diode (oled) technology: materials, devices and display technologies. *Polymer International*, 55(6):572–582, 2006.

[10] Shahul Hameed, P. Predeep, and M. R. Baiju. Polymer light emitting diodes - a review on materials and techniques. *reviews on advanced materials science*, 26:30–42, 2010.

[11] Mohamad Saleh AlSalhi, Javed Alam, Lawrence Arockiasamy Dass, and Mohan Raja. Recent advances in conjugated polymers for light emitting devices. *International Journal of Molecular Sciences*, 12(3):2036–2054, 2011. 21673938.

[12] Michael L. Chabinyc and Yueh-Lin Loo. Semiconducting polymers for thin-film electronics. *Polymer Reviews*, 46(1):1–5, 01 2006. M3: Article.

[13] R. J. Kline and M. D. McGhee. Morphology and charge transport in conjugated polymers. *Polymer Reviews*, 46(1):27–45, 01 2006. M3: Article.

[14] Jean-Luc Brédas, David Beljonne, Veaceslav Coropceanu, and Jérôme Cornil. Charge-transfer and energy-transfer processes in pi-conjugated oligomers and polymers. *Chemical Reviews*, 104(11):4971–5004, 2004. PMID: 15535639.

[15] Peter Atkins and Julio de Paula. *Atkins' Physical Chemistry*. Oxford, 7 edition, 2002.

[16] L. Akcelrud. Electroluminescent polymers. *Progress in Polymer Science*, 28(6):875–962, JUN 2003.

[17] R. H. G. Friend. Electroluminescence in conjugated polymers. *Nature*, 397(6715):121, 01/14 1999. M3: Article.

[18] N.W. Ashcroft and N.D. Mermin. *Solid State Physics*. Saunders College, Philadelphia, 1976.

[19] Charles Kittel. *Introduction to Solid State Physics*. John Wiley & Sons, Inc., New York, 6th edition, 1986.

[20] P. W. M. Blom, M. J. M. de Jong, and S. Breedijk. Temperature dependent electron-hole recombination in polymer light-emitting diodes. *Applied Physics Letters*, 71(7):930–932, August 18, 1997 1997.

[21] C. W. Tang and S. A. Vanslyke. Organic electroluminescent diodes. *Applied Physics Letters*, 51:913–915, September 1987.

[22] B. K. Crone, I. H. Campbell, P. S. Davids, and D. L. Smith. Charge injection and transport in single-layer organic light-emitting diodes. *Applied Physics Letters*, 73:3162, November 1998.

[23] P. S. Davids, S. M. Kogan, I. D. Parker, and D. L. Smith. Charge injection in organic light-emitting diodes: Tunneling into low mobility materials. *Applied Physics Letters*, 69:2270–2272, October 1996.

[24] Yong Cao, George M. Treacy, Paul Smith, and Alan J. Heeger. Solution-cast films of polyaniline: Optical-quality transparent electrodes. *Applied Physics Letters*, 60(22):2711–2713, June 1, 1992 1992.

[25] Changsheng Wang, Gun-Young Jung, Andrei S. Batsanov, Martin R. Bryce, and Michael C. Petty. New electron-transporting materials for light emitting diodes: 1,3,4-oxadiazole-pyridine and 1,3,4-oxadiazole-pyrimidine hybrids. *J. Mater. Chem.*, 12:173–180, 2002.

[26] Thuc-Quyen Nguyen, Ignacio B. Martini, Jei Liu, and Benjamin J. Schwartz. Controlling interchain interactions in conjugated polymers the effects of chain morphology on exciton-exciton annihilation and aggregation in meh-ppv films. *The Journal of Physical Chemistry B*, 104(2):237–255, 2000.

[27] Show-An Chen, Kuen-Ru Chuang, Ching-Ian Chao, and Hsun-Tsing Lee. White-light emission from electroluminescence diode with polyaniline as the emitting layer. *Synthetic Metals*, 82(3):207–210, 9/30 1996.

[28] He Yan, Paul Lee, Neal R. Armstrong, Amy Graham, Guennadi A. Evmenenko, Pulak Dutta, and Tobin J. Marks. High-performance hole-transport layers for polymer light-emitting diodes. implementation of organosiloxane cross-linking chemistry in polymeric electroluminescent devices. *Journal of the American Chemical Society*, 127(9):3172–3183, 2005.

[29] T. M. Brown, J. S. Kim, R. H. Friend, F. Cacialli, R. Daik, and W. J. Feast. Built-in field electroabsorption spectroscopy of polymer light-emitting diodes incorporating a doped poly(3,4-ethylene dioxythiophene) hole injection layer. *Applied Physics Letters*, 75(12):1679–1681, 1999.

[30] Summer R. Ferreira, Ping Lu, Yun-Ju Lee, Robert J. Davis, and Julia W. P. Hsu. Effect of zinc oxide electron transport layers on performance and shelf life of organic bulk heterojunction devices. *The Journal of Physical Chemistry C*, 115(27):13471–13475, 2011.

[31] E. Detsi, M. van de Schootbrugge, S. Punzhin, P. R. Onck, and J. T. M. De Hosson. On tuning the morphology of nanoporous gold. *Scripta Materialia*, 64(4):319–322, FEB 2011. PT: J; UT: WOS:000285951600004.

[32] Shao-Lin Mu, Yong Kong, and Jun Wu. Electrochemical polymerization of aniline in phosphoric acid and the properties of polyaniline. *Chinese Journal of Polymer Science (World Scientific Publishing Company)*, 22(5):405–415, 09 2004. M3: Article.

[33] G.G. Wallace, P.R. Teasdale, G.M. Spinks, and L.A.P. Kane-Maguire. *Conductive Electroactive Polymers: Intelligent Materials Systems, Second Edition*. Taylor & Francis, 2002.

[34] G. Inzelt and F. Scholz. *Conducting Polymers: A New Era in Electrochemistry*. Monographs in Electrochemistry. Springer, 2008.

[35] Gvozdenovic, Jugovic, Stevanovic, Trisovic, and Grgur. Electrochemical polymerization of aniline. Technical report, Faculty of Technology and Mattalurgy, University of Belgrade and Intech.

[36] A. G. Macdiarmid, J. C. Chiang, A. F. Richter, and A. J. Epstein. Polyaniline: a new concept in conducting polymers. *Synthetic Metals*, 18(1–3):285–290, 2 1987.

[37] Yinghong Xiao, Xinyan Cui, and David C. Martin. Electrochemical polymerization and properties of pedot/s-edot on neural microelectrode arrays. *Journal of Electroanalytical Chemistry*, 573(1):43–48, 11/15 2004.

[38] Andreas Elschner, Stephan Kirchmeyer, Wilfried Lovenich, Udo Merker, and Knud Reuter. *PEDOT: principles and applications of an intrinsically conductive polymer*. CRC Press, 2010.

[39] Zachary A. King, Charles M. Shaw, Sarah A. Spanninga, and David C. Martin. Structural, chemical and electrochemical characterization of poly(3,4-ethylenedioxythiophene) (pedot) prepared with various counter-ions and heat treatments. *Polymer*, 52(5):1302–1308, 3/1 2011.

[40] Yijie Xia, Kuan Sun, and Jianyong Ouyang. Solution-processed metallic conducting polymer films as transparent electrode of optoelectronic devices. *Advanced Materials*, 24(18):2436–2440, 2012.

[41] Gregory A. Sotzing, John R. Reynolds, and Peter J. Steel. Poly(3,4-ethylenedioxythiophene) (pedot) prepared via electrochemical polymerization of edot, 2,2-bis(3,4-ethylenedioxythiophene) (biedot), and their tms derivatives. *Advanced Materials*, 9(10):795–798, 1997.

[42] D. C. Look, J. W. Hemsky, and J. R. Sizelove. Residual native shallow donor in zno. *Phys. Rev. Lett.*, 82:2552–2555, Mar 1999.

[43] Anderson Janotti and de Walle Van. Hydrogen multicentre bonds. *Nat Mater*, 6(1):44–47, print 2007. M3: 10.1038/nmat1795; 10.1038/nmat1795.

[44] Jian Weng, Yongjun Zhang, Guanqi Han, Yu Zhang, Ling Xu, Jun Xu, Xinfan Huang, and Kunji Chen. Electrochemical deposition and characterization of wide band semiconductor zno thin film. *Thin Solid Films*, 478(1–2):25 – 29, 2005.

[45] J. Stejskal, P. Kratochvíl, and N. Radhakrishnan. Polyaniline dispersions 2. uv—vis absorption spectra. *Synthetic Metals*, 61(3):225–231, 12/15 1993.

[46] Cheng Gu, Teng Fei, Ming Zhang, Chuannan Li, Dan Lu, and Yuguang Ma. Electrochemical polymerization films for highly efficient electroluminescent devices and rgb color pixel. *Electrochemistry Communications*, 12(4):553–556, 4 2010.

[47] Cheng Gu, Wenyue Dong, Liang Yao, Ying Lv, Zhongbo Zhang, Dan Lu, and Yuguang Ma. Cross-linked multifunctional conjugated polymers prepared by in situ electrochemical deposition for a highly-efficient blue-emitting and electron-transport layer. *Advanced Materials*, 24(18):2413–2417, 2012.

[48] Xin Guo, Chuanjiang Qin, Yanxiang Cheng, Zhiyuan Xie, Yanhou Geng, Xiabin Jing, Fosong Wang, and Lixiang Wang. White electroluminescence from a phosphonate-functionalized single-polymer system with electron-trapping effect. *Advanced Materials*, 21(36):3682–3688, 2009.

[49] Baohua Zhang, Chuanjiang Qin, Junqiao Ding, Lei Chen, Zhiyuan Xie, Yanxiang Cheng, and Lixiang Wang. High-performance all-polymer white-light-emitting diodes using polyfluorene containing phosphonate groups as an efficient electron-injection layer. *Advanced Functional Materials*, 20(17):2951–2957, 2010.

[50] Ke Wang and Jörg Weissmüller. Composites of nanoporous gold and polymer. *Advanced Materials*, 25(9):1280–1284, 2013.

[51] A. C. Fou, O. Onitsuka, M. Ferreira, M. F. Rubner, and B. R. Hsieh. Fabrication and properties of light-emitting diodes based on self-assembled multilayers of poly(phenylene vinylene). *Journal of Applied Physics*, 79(10):7501–7509, 1996.

[52] T. Piok, C. Brands, P. J. Neyman, A. Erlacher, C. Soman, M. A. Murray, R. Schroeder, W. Graupner, J. R. Heflin, D. Marciu, A. Drake, M. B. Miller, H. Wang, H. Gibson, H. C. Dorn, G. Leising, M. Guzy, and R. M. Davis. Photovoltaic cells based on ionically self-assembled nanostructures. *Synthetic Metals*, 116(1–3):343–347, 1/1 2001.

[53] Dongsik Yoo, Jin-kyu Lee, and M. F. Rubner. Investigations of new self-assembled multilayer thin films based on alternately adsorbed layers of polyelectrolytes and functional dye molecules. *MRS Proceedings*, 413, 1 1995.

[54] E. T. Faber, D. Martinez-Martinez, C. Mansilla, V. Ocelik, and J. Th M. De Hosson. Calibration-free quantitative surface topography reconstruction in scanning electron microscopy. *To be published*.

[55] Bernd Minnich and Alois Lametschwandtner. Lengths measurements in microvascular corrosion castings: Two-dimensional versus three-dimensional morphometry. *Scanning*, 22(3):173–177, 2000.

[56] Jiejun Zhu, Caixia Kan, Xiaoguang Zhu, Jian guo Wan, Min Han, Yue Zhao, Baolin Wang, and Guanghou Wang. Synthesis of perfect silver nanocubes by a simple polyol process. *Journal of Materials Research*, 22(06):1479–1485, 6 2007.

[57] Dongjo Kim and Jooho Moon Sunho Jeong and. Synthesis of silver nanoparticles using the polyol process and the influence of precursor injection. *Nanotechnology*, 17(16):4019, 2006.

[58] Benjamin Wiley, Yugang Sun, Brian Mayers, and Younan Xia. Shape-controlled synthesis of metal nanostructures: The case of silver. *Chemistry ? A European Journal*, 11(2):454–463, 2005.

[59] Hongyan Liang, Wenzhong Wang, Yingzhou Huang, Shunping Zhang, Hong Wei, and Hongxing Xu. Controlled synthesis of uniform silver nanospheres. *The Journal of Physical Chemistry C*, 114(16):7427–7431, 04/29; 2013/09 2010. doi: 10.1021/jp9105713; M3: doi: 10.1021/jp9105713; 25.

[60] YugangXia Sun Younan. Shape-controlled synthesis of gold and silver nanoparticles. *Science*, 298(5601):2176–2179, 12/13 2002. M3: Article.

[61] Rosa E. Davila-Martinez, Luisa F. Cueto, and Eduardo M. Sanchez. Electrochemical deposition of silver nanoparticles on tio2/fto thin films. *Surface Science*, 600(17):3427 – 3435, 2006.